Catal Lett (2013) 143:673–680
DOI 10.1007/s10562-013-1010-x

Highly Active Hydroformylation Catalysts: Synthesis, Characterisation and Catalytic Performance

Elisabetta Piras · Bernhard Powietzka · Frederik Wurst · Doreen Neumann-Walter · Hans-Jörg Grützmacher · Thomas Otto · Thomas Zevaco · Olaf Walter

Received: 7 March 2013 / Accepted: 14 April 2013 / Published online: 15 May 2013

Abstract The phoszone ligand [(Ph_2P)(bis-3,5-CF_3-Ph)]NN=CH(penta-fluoro-Ph) transformed in liquid CO_2 at room temperature in presence of [Rh(cod)$_2$]OTf into [Rh(cod)(η^2-P,P′-Ph_2POPPh_2)]OTf. Replacing the O-atom in Ph_2POPPh_2 by a PrN-group leads to the ligand PrN(PPh_2)$_2$ acting similarly as a bidentate ligand in [Rh(cod)(η^2-P,P′-PrN(PPh_2)$_2$)]OTf. Hydroformylation of 1-octene with in situ catalysts formed by the ligands with [Rh(cod)$_2$]OTf showed hydroformylation activities at 50 % conversion of 16,000 h^{-1} (PrN(PPh_2)$_2$/[Rh(cod)$_2$]OTf) and 24,000 h^{-1} (phoszone/[Rh(cod)$_2$]OTf), respectively.

Keywords Homogeneous catalysis · Activity · Hydroformylation · Isomerisation

1 Introduction

Hydroformylation is one of the best studied catalytic reactions [1, 2]. However, only few highly active catalysts are known in the literature [3–10]. The phoszone ligand **1** bearing fluorinated side chains (Fig. 1) forms in the presence of [Rh(cod)$_2$]OTf or [Rh(cod)$_2$]BF_4 an in situ Rh-catalyst with an exceptionally high activity in the hydroformylation of 1-octene [11]. Already the introduction of some fluorinated positions in the ligands of metal complexes could increase the solubility of the pre-catalyst in supercritical carbon dioxide [12]. Therefore it seemed logical to studying the activity of the Rh-complexes of the phoszone ligand **1** in supercritical carbon dioxide offering the possibility by the use of this solvent to enhance the reactivity further [13, 14]. This could have been well the case as for highly active catalysts in the more phase hydroformylation mass transfer could become the rate limiting step which could be overcome by the application of supercritical carbon dioxide as the solvent creating a single phase system [13, 14]. In this publication we describe how experiments with the phoszone ligand **1** lead to the development of highly active Rh-catalysts for the hydroformylation of 1-octene.

2 Results and Discussion

Preliminary hydroformylation experiments with an in situ catalyst system containing the ligand **1** and [Rh(cod)$_2$]OTf as the pre-catalyst showed a very high catalytic activity with tofs of more than 20,000 h^{-1} [11]. Our attempts to study the complex chemistry of the ligand **1** towards Rh-complex fragments present in [Rh(cod)$_2$]OTf or [Rh(cod)$_2$]BF_4 under reaction conditions turned out to be difficult: A complex mixture of products was obtained proven by ^{31}P NMR. In order to reduce the number of phases in the system we wanted to investigate the reaction in sc CO_2 by HP NMR. Therefore NMR studies in dense carbon dioxide were prepared: two equivalents (0.02 mmol) of the ligand **1**, 1 eq. of [Rh(cod)$_2$]OTf and liquid carbon dioxide (1 ml) were introduced in a HP NMR tube for further investigations the next day. Over night single crystals precipitated in the NMR

Dedicated to the memory of Prof. Ivano Bertini.

E. Piras · B. Powietzka · F. Wurst · D. Neumann-Walter · T. Otto · T. Zevaco · O. Walter (✉)
IKFT, Campus Nord, KIT, Hermann-von-Helmholtz-Platz 1, 76344 Eggenstein-Leopoldshafen, Germany
e-mail: olaf.walter@kit.edu

E. Piras · H.-J. Grützmacher
Laboratorium für Anorganische Chemie, Wolfgang-Pauli-Street. 10, ETH Hönggerberg, HCI H 131, 8093 Zurich, Switzerland

tube of other shape than the pure [Rh(cod)$_2$]OTf. The NMR tube was depressurised and the crystals were isolated and a single crystal xray diffraction analysis was performed.

The result from the xray analyses showed the constitution of the complex to be [Rh(cod)(η^2-P,P′-Ph$_2$POPPh$_2$)](OTf) (**2***OTf, Fig. 2) without any direct coordination of the ligand **1** to the Rh(cod)-complex fragment but with a η^2-P,P′-coordination of the POP-ligand Ph$_2$POPPh$_2$. Concerning its structural characteristics the geometry of the Rh-center in the complex cation **2** can be described as distorted square planar taking the center of the coordinated CC bonds as their center of gravity. The Rh–P–O–P four ring is planar (mean $\sigma = 0.46$ pm from the plane) with a small P-Rh-P angle of 68.7° at the Rh atom resulting from the four ring formation. This structural feature is typical for complexes where a transition metal is embedded in a 4-membered ring with two phosphino-groups coordinating to the metal bridged over an oxygen atom [15–20].

It seems reasonable to assume that **2***OTf and therefore the POP ligand Ph$_2$POPPh$_2$ in the cation **2** is formed by partial hydrolysis of the ligand **1** in the coordination sphere of the metal according to the literature [15–20]; alternatively carbon dioxide could have functioned as the oxygen source [21]. In the small amount of carbon dioxide present in this HP NMR experiment the ligand **1** is already transformed in that way that crystallisation of **2***OTf proceeds. So it should be obvious that under real catalytic conditions in presence of higher amounts of carbon dioxide and other chemicals the ligand **1** and Rh-precursor would be transformed even easier. If furthermore the formation of Ph$_2$POPPh$_2$ proceeds already at RT then it should proceed at elevated temperature even faster. Therefore it might be possible that the catalytically active species in the hydroformylation of 1-octene involving the phoszone **1** as the stabilising ligand is in all cases formed by Rh-complexes stabilised by coordination to a Ph$_2$POPPh$_2$-ligand.

The ligand Ph$_2$POPPh$_2$ itself is not easily available, and a further functionalisation can be introduced only in the substituents at the P-atoms. So our idea at this point was addressed to the application of the isolobal-principle [22] and therefore to replace the O-atom in the POP-ligand

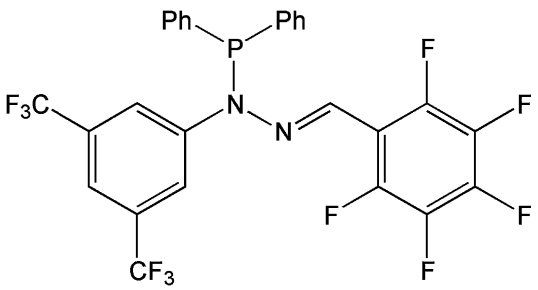

Fig. 1 The phoszone ligand **1** from the Grützmacher's group

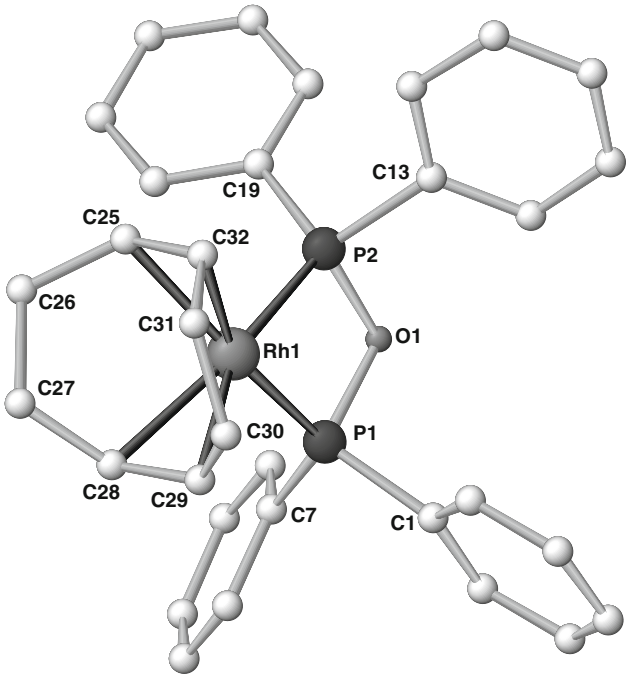

Fig. 2 View to the molecular structure of one of the two independent cations of **2** in the crystal, H atoms, triflate anion and numbering of C-atoms in the aromatic rings omitted due to reasons of clarity. Selected bond lengths [pm] and angles [°] for both independent molecule cations: Rh-P: 222.83(6), 223.48(6), 223.82(6), 224.79(6); Rh1-C (cod): 224.5(2), 224.9(2), 226.9(2), 227.0(2), 227.2(2), 228.0(2), 228.3(2), 229.0(2); P-O: 166.35(16), 166.71(16), 167.05(16), 167.10(16); P-Rh-P: 68.71(2), 68.78(2); Rh-P-O: 95.92(6), 96.28(6), 96.52(6), 96.86(6); P-O-P: 98.38(8), 98.51(8)

Ph$_2$POPPh$_2$ in **2** by an isoelectronical NR-group leading to ligands of the type RN(PR′$_2$)$_2$. These ligands are more easily accessible and accordingly many of their transition complexes are known in the literature [23–26] but only very few Rh-complexes are reported [27, 28]. Functionalisation enabling e.g. an immobilisation of these ligands can relatively easily be achieved at the substituent directly linked to the N-atom [29].

We synthesised the ligand PrN(PPh$_2$)$_2$ (**3**) by reaction of PrNH$_2$ with two equivalents of ClPPh$_2$ in presence of NEt$_3$, and the ligand could be isolated after purification in 85 % yield according to [30–32]. Further reaction of one equivalent of the ligand with [Rh(cod)$_2$]OTf lead to the nearby quantitative formation of the complex [Rh(cod)(η^2-P,P′-PrN(PPh$_2$)$_2$)](OTf) of which from CDCl$_3$ solution a single crystal was isolated being consistent with **4***OTf*CDCl$_3$ (Fig. 3).

In the cation **4** the geometry at the Rh center can be described as distorted square planar due to the η^2-P,P′-coordination of the ligand PrN(PPh$_2$)$_2$. Like the O-atom in **2** the N-atom in **4** is part of the four membered planar Rh–P–N–P ring (mean deviation from the plane = 0.8 pm). The overall structural features of **4** show a general high

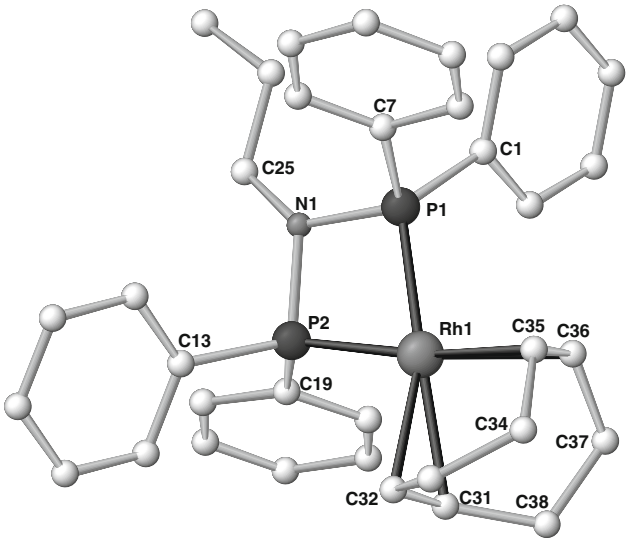

Fig. 3 View to the molecular structure of **4***OTf*$CDCl_3$ in the crystal, H atoms, triflate anion, solvent molecules and numbering of C-atoms in the aromatic rings and the side chains omitted due to reasons of clarity. Selected bond lengths [pm] and angles [°]: Rh-P: 224.0(1), 225.7(1); Rh1-C (cod): 223.4(3), 224.3(3), 225.8(3), 228.6(3); P-N: 170.7(3), 170.8(3); P-Rh-P: 70.51(3); Rh-P-N: 94.93(9), 95.59(9); P-N-P: 98.95(14)

similarity and comparability to the bonding of the ligand Ph_2POPPh_2 in the cation **2**. Accordingly due to the embedding of the Rh-atom in the four membered ring system the P–Rh–P bond angle is with 70.5° small; and relatively short Rh–N distances are observed (291.2 and 291.5 pm, respectively, versus a Rh–O distance of 293.6 pm in **2**) enabling a certain through space interaction between those atoms [33].

Due to the generally high congruence in the structural data of the cations **2** and **4** we expect comparable catalytic features for Rh-complexes stabilised by Ph_2POPPh_2 or $PrN(PPh_2)_2$. Under the reaction conditions it is in agreement with the literature very likely that from $[Rh(cod)_2]OTf$ in the presence of Ph_2POPPh_2 or $PrN(PPh_2)_2$ the catalytically active complexes $[Rh(H)(\eta^2\text{-}P,P'\text{-}Ph_2POPPh_2)(CO)_2]$, or $[Rh(H)(\eta^2\text{-}P,P'\text{-}PrN(PPh_2)_2)(CO)_2]$ are formed, respectively [34, 35]. Accordingly, here hydroformylation experiments are presented with an si-situ catalyst formed from the $[Rh(cod)_2]OTf$ and $PrN(PPh_2)_2$ (Table 1, entries 1–4). Additionally, results are presented using an in situ catalyst prepared from the phoszone ligand **1** and appropriate amounts of $[Rh(cod)_2]OTf$ (Table 1, entry 5) and the pre-catalyst $[(\eta^2\text{-}P,P'\text{-}PrN(PPh_2)_2)Rh(acac)]$ (Table 1, entry 6), respectively. The catalytic experiments are performed at different pressures at 100 °C as at lower temperatures the catalysts show a considerably lower activity. Kinetic concentrations versus time profiles are obtained by sampling followed by GC-fid analyses (Figs. 4, 5, 6, 7, 8, 9; Table 1).

In this paper only the first results on hydroformylation experiments are presented. The reactions are performed in pure 1-octene leading to an initial 1-octene concentration of ~6.42 mol/l or in thf/1-octene mixtures so that the in Table 1 presented concentrations are reached. By this approach catalytic experiments with very high substrate to metal ratios of more than 100,000 could be performed. Comparing the concentration versus time profiles it can be noted that the system is highly active in both terms of hydroformylation and isomerisation (Figs. 4, 5, 6, 7, 8, 9). In the reaction mixtures analysed different octene derivatives and their hydroformylation products are observed. The intermediates or products produced in most significant amounts are 2-octene, nonanal, and 2-methyloctanal, respectively. During the reaction progress all the starting material (1-octene) is consumed, turnover numbers (ton) equal to the substrate to metal ratio are obtained in all experiments (s/m-ratio, Table 1).

In the meantime an immobilised catalyst system is developed and tested [36]. An alternative approach involving magnetic nano-particles for catalyst separation has been developed [37]. Reactions in sc CO_2 have been performed [38] as well as more detailed kinetic investigations on a series of Rh-complexes stabilised with ligands of the type $RN(PPh_2)_2$ [39]. These results will be subject of future publications; whereas this contribution is focused on the discovery and the description of first catalytic experiments which are discussed in detail now.

Generally in all experiments the product distribution obtained can be explained by two parallel ongoing processes in agreement with the in the literature discussed mechanisms [40, 41]: isomerisation and hydroformylation leading to mixtures of isomeric octenes and C9-aldehydes (Fig. 10); hydrogenation is practically not observed. In all experiments the concentrations versus time profiles show common behaviours: the concentration of 2-octene in the reaction mixture increases by the time and - after having reached a maximum - it decreases in the following period (Table 1; Figs. 4, 5, 6, 7, 8, 9). Accordingly the 1-octene concentration decreases rapidly at the beginning of the reactions, it is consumed by the isomerisation to 2-octene and the hydroformylation to nonanal and/or 2-methyloctanal. Once after significant amounts of 2-octene are present in the reaction mixture one possible isomerisation product of 2-octene, namely 3-octene, is formed in observable concentrations. Hydroformylation proceeds anyway at the same time which is reflected in the by time increasing concentrations of nonanal and 2-methyloctanal. After the 1-octene in the reaction mixture is nearby completely consumed but considerable amounts of 2-octene are still present the hydroformylation of 2-octene proceeds and as a result the 2-methyloctanal formation rate becomes predominant over the one for nonanal. Accordingly for all experiments the

Table 1 Comparison of the hydroformylation experiments

Run, fig	p (bar)	c (cat) (mmol/l)	c (lig) (mmol/l)	s/m-ratio	tof_{50} (h^{-1})	$S_{nonanal}$ (%)	$S_{2\text{-}mo}$ (%)	$S_{2\text{-}o}$ (%)	$S_{3\text{-}o}$ (%)	$tof_{50/HF}$ (h^{-1})	$tof_{50/Iso}$ (h^{-1})
1, 4	40	0.0379	0.045	169,600	13,510	11.5	2.7	81.5	4.3	1,920	11,580
2, 5	54	0.0339	0.038	189,800	19,470	22.9	7.5	66.4	3.0	5,920	13,510
3, 6	40	0.0318	0.041	67,300	50,500	14.6	4.3	76.5	4.5	9,545	40,900
4, 7	120	0.0271	0.037	118,600	25,780	44.6	17.8	36.2	1.2	16,090	9,640
5, 8	120	0.0270	0.075	119,000	37,660	45.8	18.5	34.1	1.4	24,210	13,370
6, 9	125	0.0405	0.0405	122,700	57,000	45.1	18.6	35.3	0.8	36,300	20,600

T: 100 °C. s/m-ratio: substrate to metal ratio. All selectivities (S) calculated for 50 % conversion. $S_{2\text{-}mo}$: Selectivity 2-methyloctanal. $S_{2\text{-}o}$: Selectivity towards cis and trans 2-octene. $S_{3\text{-}o}$: Selectivity towards cis and trans 3-octene. All not mentioned products are detectable only in traces. tof_{50} refers to the activity at 50 % conversion, $tof_{50/HF}$ to the hydroformylation activity, and $tof_{50/Iso}$ to the isomerisation activity at 50 % conversion. Entries 1–3 carried out in 200 ml of pure 1-octene (c_0 = 6.428 mol/l), the other entries are diluted with thf according to s/m-ratio. Entry 5 has been performed with the phoszone ligand **1**, in all other experiments $PrN(PPh_2)_2$ (**3**) as the ligand was used. In entry 6 the complex [(η^2-P,P′-$PrN(PPh_2)_2$)Rh(acac)] was used as the pre-catalyst

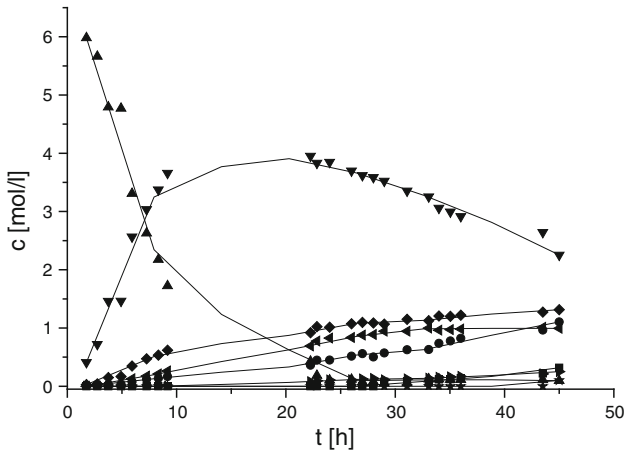

Fig. 4 concentration versus time curve for a hydroformylation experiment of 1-octene with an situ-catalyst formed from [Rh(cod)$_2$]OTf and $PrN(PPh_2)_2$. P = 40 bar. c_0(cat) = 0.0000379 mol/l, c_0(1-octene) = 6.428 mol/l ([1-octene]/[Rh] (at t = 0 h) = 169,600). *Filled triangle*: 1-octene, *filled inverse triangle*: 2-octene, *left pointing filled triangle*: 3-octene, *right pointing filled triangle*: 4-octene, *filled diamond*: nonanal, *filled circle*: 2-methyloctanal, *filled square*: 2-ethylheptanal, *filled star*: 2-propylhexanal

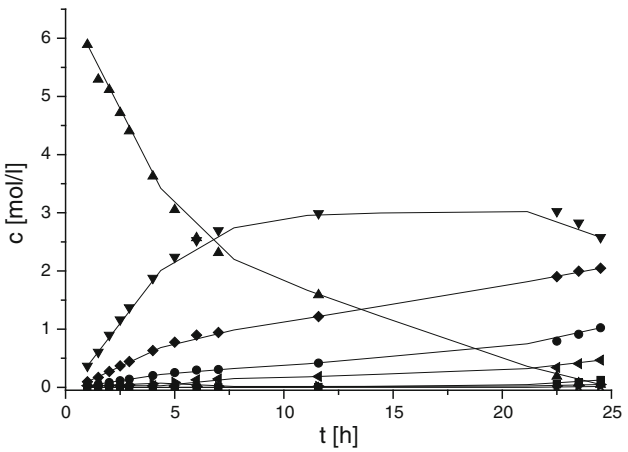

Fig. 5 concentration versus time curve for a hydroformylation experiment of 1-octene with an situ-catalyst formed from [Rh(cod)$_2$]OTf and $PrN(PPh_2)_2$. P = 54 bar. c_0(cat) = 0.00003387 mol/l, c_0(1-octene) = 6.428 mol/l ([1-octene]/[Rh] (at t = 0 h) = 189,800). *Filled triangle*: 1-octene, *filled inverse triangle*: 2-octene, *left pointing filled triangle*: 3-octene, *right pointing filled triangle*: 4-octene, *filled diamond*: nonanal, *filled circle*: 2-methyloctanal, *filled square*: 2-ethylheptanal, *filled star*: 2-propylhexanal

n/i-ratio changes by the time: at 50 % conversion n/i-ratios are found in the range between 2.5 (entries 4, 5, 6, Table 1) and 4 (entry 1 but with low hydroformylation activity) whereas at the end of the reaction (nearby complete olefine consumption) they are determined in the range between 1 and 2 (Figs. 4, 5, 6, 7, 8, 9).

For evaluating the data closer as reference the data at 50 % conversion are taken as they are representative and not deviated from low or already very high conversions. tof_{50} represents the tof at 50 % and with respect to the selectivity the $tof_{50/HF}$ the hydroformylation activity of the catalyst at 50 % conversion, and the $tof_{50/iso}$ reflects its isomerisation activity, all at 50 % conversion, respectively (Table 1).

In the experiments at lower pressures the isomerisation activity of the catalyst is significantly higher (up to six times) than its hydroformylation activity (Table 1: entries 1–3, Fig. 4, 5, 6). This is reflected in higher concentration of 2-octene as the preliminary isomerisation product compared to the corresponding sum of the concentrations of the aldehydes formed. Accordingly in these experiments the concentration of 2-octene in the reaction mixture remains high over the whole reaction course: in the same magnitude as the one of *n*-nonanal. A significant pressure influence on the selectivity is observed: increasing the pressure to 120 bar the hydroformylation activity of the system becomes approximately two times higher than its isomerisation activity (Table 1). If the pressure is increased

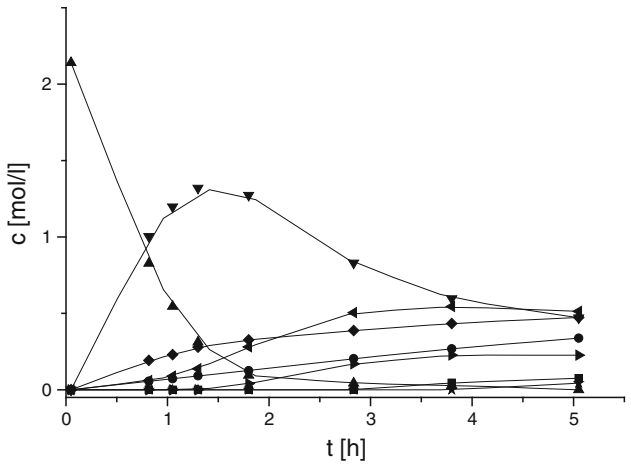

Fig. 6 concentration versus time curve for a hydroformylation experiment of 1-octene with an situ-catalyst formed from [Rh(cod)$_2$]OTf and PrN(PPh$_2$)$_2$. $P = 40$ bar. c_0(cat) = 0.0000318 mol/l, c_0(1-octene) = 2.14 mol/l ([1-octene]/[Rh] (at t = 0 h) = 67,300). *Filled triangle*: 1-octene, *filled inverse triangle*: 2-octene, *left pointing filled triangle*: 3-octene, *right pointing filled triangle*: 4-octene, *filled diamond*: nonanal, *filled circle*: 2-methyloctanal, *filled square*: 2-ethylheptanal, *filled star*: 2-propylhexanal

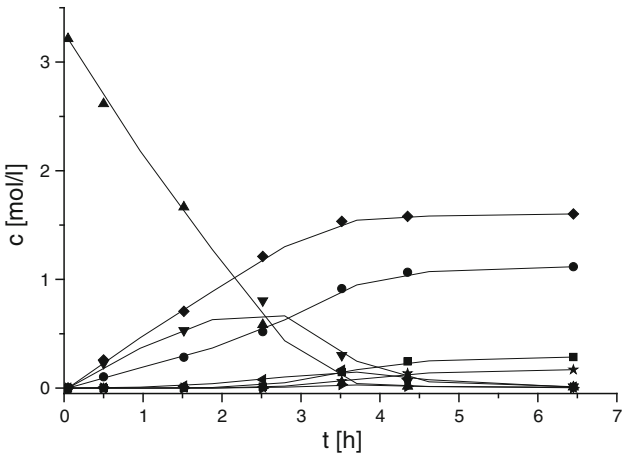

Fig. 8 concentration versus time curve for a hydroformylation experiment of 1-octene with an situ-catalyst formed from [Rh(cod)$_2$]OTf and the phoszone **1**. $P = 120$ bar. c_0(cat) = 0.000027 mol/l, c_0(1-octene) = 3.214 mol/l ([1-octene]/[Rh] (at t = 0 h) = 119,000). *Filled triangle*: 1-octene, *filled inverse triangle*: 2-octene, *left pointing filled triangle*: 3-octene, *right pointing filled triangle*: 4-octene, *filled diamond*: nonanal, *filled circle*: 2-methyloctanal, *filled square*: 2-ethylheptanal, *filled star*: 2-propylhexanal

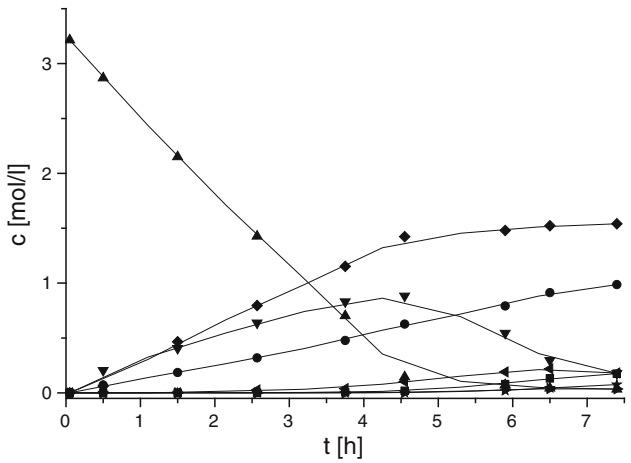

Fig. 7 concentration versus time curve for a hydroformylation experiment of 1-octene. $P = 120$ bar with an situ-catalyst formed from [Rh(cod)$_2$]OTf and PrN(PPh$_2$)$_2$. c_0(cat) = 0.0000271 mol/l, c_0(1-octene) = 3.214 mol/l ([1-octene]/[Rh] (at t = 0 h) = 118,600). *Filled triangle*: 1-octene, *filled inverse triangle*: 2-octene, *left pointing filled triangle*: 3-octene, *right pointing filled triangle*: 4-octene, *filled diamond*: nonanal, *filled circle*: 2-methyloctanal, *filled square*: 2-ethylheptanal, *filled star*: 2-propylhexanal

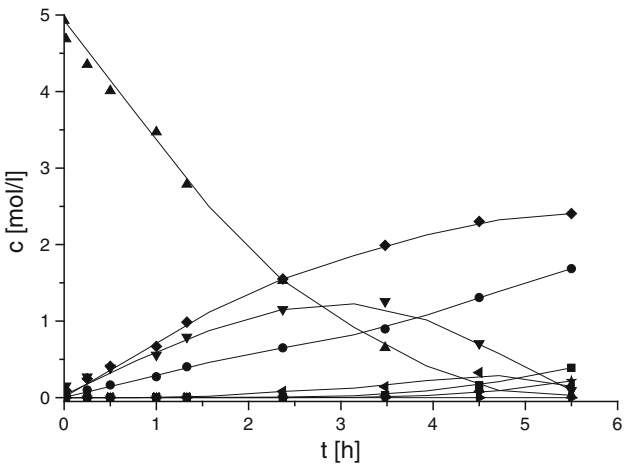

Fig. 9 concentration versus time curve for a hydroformylation experiment of 1-octene. $P = 125$ bar. Pre-cat.: [(PrN(PPh$_2$)$_2$)Rh(acac)]. c_0(cat) = 0.0000405 mol/l, c_0(1-octene) = 4.973 mol/l ([1-octene]/[Rh] (at t = 0 h) = 122,700). *Filled triangle*: 1-octene, *filled inverse triangle*: 2-octene, *left pointing filled triangle*: 3-octene, *right pointing filled triangle*: 4-octene, *filled diamond*: nonanal, *filled circle*: 2-methyloctanal, *filled square*: 2-ethylheptanal, *filled star*: 2-propylhexanal

to more than 160 bar the reaction rate drops again. This pressure influence could be explained by the assumption that at lower pressure the concentration of syngas in the reaction mixture is lower and therefore the corresponding reaction rate involving syngas as the substrate (the hydroformylation) is lower as well. So the hydroformylation raction rate is influenced positively by a pressure increase. This pressure influence is not seen for the isomerisation, so its reaction rate does not show a real pressure influence. These findings are confirmed by all the experiments reported (Figs. 4, 5, 6, 7, 8, 9); Table 1): e.g. comparing the first two entries (Table 1) at 40 and 54 bar pressure but under otherwise identical conditions one can see that the hydroformylation activity is positively influenced by the

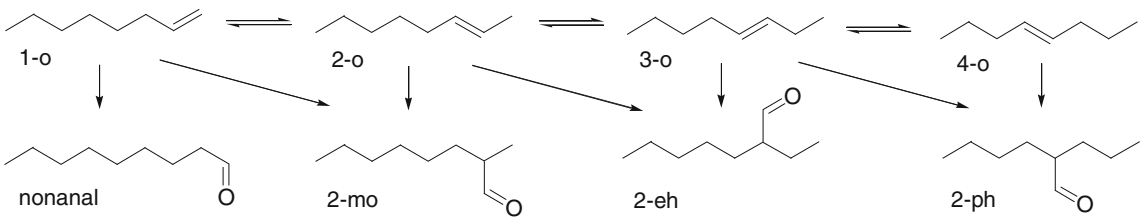

Fig. 10 isomerisation and hydroformylation products of 1-octene, overview. 1-o: 1-octene. 2-o: 2-octene. 3-o: 3-octene. 4-o: 4-octene. 2-mo: 2-methyloctanal. 2-eh: 2-ethylheptanal. 2-ph: 2-propylhexanal

pressure increase whereas the isomerisation activity shows only a slight increase. This results in a better selectivity towards the hydroformylation products in the reaction mixture.

Experiments 3, 4 and 5 (Table 1) are executed in thf/1-octene mixtures leading to lower 1-octene concentrations compared to the experiments 1, 2 and 6. This leads to a different polarity in the system which seems to effect the activity positively. Accordingly in entry 3 with the highest thf concentration the highest activity of the whole system is observed while the selectivity remains comparable to the experiments performed at the same pressure.

Comparing entries 4, 5 in Table 1 a difference in the catalyst system can be noted: in entry 4 $PrN(PPh_2)_2$ (**3**) was used as the stabilising ligand whereas in entry 5 the pure phoszone ligand **1** was present in the reaction mixture under otherwise very similar conditions (but with respect that two moieties of **1** might be transformed into one molecule of Ph_2POPPh_2). The presence of the phoszone ligand **1** instead of the prepared $PrN(PPh_2)_2$ (**3**) leads to a higher activity of the system. The selectivity in the Rh-catalysed hydroformylation of 1-octene is in both cases comparable. This could be explained by the similar structural features of the two ligands in the Rh-coordination sphere, while their electronically different features then cause the different activity.

However, to our opinion the overall similarity of the catalytical behaviour of the two ligands in the catalysis is a strong sign that the finally catalytically active complex in the Rh-catalysed hydroformylation of 1-octene involving the phoszone **1** is a complex with the Ph_2POPPh_2 ligand in the coordination sphere of the transition metal. This was the motivation of our studies here showing that the ligand $PrN(PPh_2)_2$ in the Rh-catalysed hydroformylation of 1-octene leads to high activity as well.

Indeed changing the pre-catalyst from an ionic in situ system (formed from $[Rh(cod)_2]OTf$ and $PrN(PPh_2)_2$) to the neutral pre-catalyst $[(\eta^2\text{-P,P}'\text{-PrN}(PPh_2)_2)Rh(acac)]$ this influences on the activity (entry 6, Table 1; Fig. 9). A significantly enhanced activity can be obtained with with a tof_{50} of $\sim$57,000 h^{-1} realised with the ligand $PrN(PPh_2)_2$. The selectivity remains comparable to all other experiments at this pressure (Table 1).

3 Conclusion

We show that the phoszone ligand **1** is easily transformed into the POP ligand Ph_2POPPh_2 which has been proven by xray analysis of the complex $[Rh(cod)(\eta^2\text{-P,P}'\text{-}Ph_2POPPh_2)](OTf)$ (**2***OTf). We assume that complexes of the type $[Rh(H)(\eta^2\text{-P,P}'\text{-}Ph_2POPPh_2)(CO)_2]$ form the catalytically active species in the hydroformylation of 1-octene when the phoszone ligand **1** is involved. As POP ligands are not easily accessible we prepared the corresponding PNP ligand $PrN(PPh_2)_2$ (**3**), showed its η^2-P,P′-coordination behaviour in the complex $[Rh(cod)(\eta^2\text{-P,P}'\text{-PrN}(PPh_2)_2)]$ (OTf) (**4***OTf), and tested it as an in situ system as well in the hydroformylation of 1-octene. A pressure dependency in the system $PrN(PPh_2)_2/[Rh(cod)_2]OTf$ is observed according to its high activity and showing enhanced hydroformylation activity at pressures up to 140 bar.

The results show that the system $PrN(PPh_2)_2/[Rh(cod)_2]OTf$ generally agrees in terms of catalytic selectivity and activity with the one obtained from the phoszone **1** and $[Rh(cod)_2]OTf$ being a sign for structural and electronic comparability of the active catalyst. Both systems show high hydroformylation activity with tof_{50} up to 25,000 h^{-1}. Activity can be further increased by changing the pre-catalyst nature from ionic to neutral: with $[(\eta^2\text{-P,P}'\text{-PrN}(PPh_2)_2)Rh(acac)]$ as pre-catalyst a hydroformylation tof_{50} of 36,300 h^{-1} is obtained at identical selectivity for the same pressure.

As the catalyst is not only a hydroformylation but as well an effective isomerisation catalyst it seems to be promising to perform as well more extended investigation on combined isomerisation hydroformylation experiments with sterically hindered olefins as the substrate. Furthermore immobilisation of the catalyst system is under research towards the development of a continuously driven hydroformylation process for higher olefins.

4 Experimental

4.1 Materials and Methods

All preparations were carried using standard Schlenk techniques. Preparation of $PrN(PPh_2)_2$ (**3**) was performed

according to [30]. The catalytic experiments in this publication were performed in a 300 ml autoclave. Prior to the experiment the autoclave was pressurised three times with N_2 and the pressure was released in order to inert the system. The catalyst was filled into the autoclave together with the substrate and—if desired—some additional solvent and the system was heated up to the reaction temperature while pressurising to the required pressure. The time when the reaction temperature was reached was taken as t_0. Samples were taken and applied to GC analyses (HP 5830).

NMR analyses were performed on a Bruker AVANCE 250 NMR system. XRD measurements were performed on Siemens SMART CCD 1000 diffractometer with monochromated MoKα-irradiation collecting a full sphere of data in the θ–range from 1.57 to 28.34°. Frames were collected with an irradiation time of 6 s (**2***OTf) or 40 s (**4***OTf*$CDCl_3$) per frame and ω–scan technique with $\Delta\omega = 0.45°$.[1] Data were corrected to Lorentz and polarisation effects and an empirical adsorption correction with sadabs [42] was applied. The structures were solved by direct methods and refined to an optimum R_1 value with SHELX-97 [43]. Visualisation for evaluation was performed with xpma [44] and figures were created with winray [45]. The structures have been deposited at the CCDC referring to the CCDC numbers 915597 (**2**) and 915598 (**4**).

4.1.1 Preparation of 2*OTf

Single crystals of [Rh(cod)(η^2-P,P′-Ph_2POPPh_2)](OTf) (**2***OTf, Fig. 2) were obtained overnight from a solution of 0.02 mmol of the ligand **1** and 0.01 mmol of [Rh(cod)$_2$]OTf and liquid carbon dioxide (1 ml) inside a HP NMR tube. Details of the single crystal analyses see footnote 1. No further analytical data can be provided.

4.1.2 Preparation of 4*OTf

468.3 mg (1.0 mmol) of [Rh(cod)$_2$](OTf) were dissolved in 20 ml of CH_2Cl_2, a solution of 427.5 mg (1.0 mmol) $PrN(PPh_2)_2$ in 20 ml of CH_2Cl_2 was added and the solution was stirred for 30 min at RT. The solvent was removed in vacuum and the residual solid washed three times with 10 ml of Et_2O and pentane, successively, and dried in vacuum. 733.1 mg (0.93 mmol, 93 %) of [Rh(cod)(η^2-P,P′-$PrN(PPh_2)_2$)](OTf) (**4***OTf) were isolated of which single crystal were obtained from a solution of the **4***OTf in $CDCl_3$ being of the consistence **4***OTf*$CDCl_3$. Details of the single crystal analyses see footnote 1.

^{1}H ($CDCl_3$) δ/ppm = 7.8–7.4 (m, 20H, aromatic protons), 5.21 (s, 4H, coordinated cod CH), 2.72 (m, 2H, NCH_2), 2.4 (s, br, 8H, cod CH_2), 1.03 (m, 2H, $CH_2\underline{CH_2}CH_3$), 0.43 (t, $^3J_{H-H}$ = 7.2 Hz, 3H, CH_3).

$^{13}C\{^1H\}$ ($CDCl_3$) δ/ppm = 135.0, 133.6, 130.4, 128.7 (aromatic C), 118.0 (coordinated cod C), 35.7 (NCH_2), 28.1 (cod CH_2), 27.0 ($CH_2\underline{CH_2}CH_3$), 11.3 (CH_3).

$^{31}P\{^1H\}$ ($CDCl_3$) δ/ppm = 52.1 (d, $^1J_{P-Rh}$ = 136.2 Hz).

$C_{36}H_{39}F_3NO_3P_2RhS$, calc. (%): C 54.90; H 4.99; F 7.24; N 1.78; O 6.09; P 7.87; Rh 13.07; S 4.07—found (%): C 55.13; H 5.16; N 1.91, S 4.19.

4.1.3 Preparation of [PrN(PPh2)2Rh(acac)]

258 mg (1.0 mmol) of [$(CO)_2$Rh(acac)] were dissolved in 10 ml of CH_2Cl_2, a solution of 427 mg (1.0 mmol) $PrN(PPh_2)_2$ in 20 ml of CH_2Cl_2 was added and the solution was stirred for 30 min at RT. The solvent was removed in vacuum and the residual solid washed three times with 10 ml of Et_2O and pentane, successively, and dried in vacuum. 550 mg (0.92 mmol, 92 %) of [($PrN(PPh_2)_2$)Rh(acac)] were isolated.

^{1}H ($CDCl_3$) δ/ppm = 8.0–7.0 (m, 20H, aromatic protons), 5.51 (s, 1H, COCHCO), 2.72 (m, $^3J_{H-H}$ = 8.3 Hz, $^3J_{P-H}$ = 5.8 Hz, 2H, NCH_2), 1.07 (tq, $^3J_{H-H}$ = 7.8 Hz, $^3J_{H-H}$ = 7.2 Hz, 2H, $CH_2\underline{CH_2}CH_3$), 0.44 (t, $^3J_{H-H}$ = 7.3 Hz, 3H, CH_3).

$^{31}P\{^1H\}$ ($CDCl_3$) δ/ppm = 71.6 (d, $^1J_{P-Rh}$ = 122.9 Hz).

$C_{32}H_{34}NO_2P_2Rh$, calc. (%): C 61.06; H 5.44; N 2.23; O 5.08; P 9.84; Rh 16.35—found (%): C 62.17; H 5.82; N 2.42.

Acknowledgment The authors would like to express their deepest thanks to the KIT and the ETH Zürich for the financial and Prof. Dr. Eckhard Dinjus for the general support of this work.

References

1. Franke R, Selent D, Börnera A (2012) Chem Rev 112:5675
2. Ungvary F (2007) Coord Chem Rev 251:2072

[1] Structural details for **2***OTf: Reflections collected/unique/observed ($I > 2\sigma$): 40,467/15,873/12,529 [R(int) = 0.222]; parameters refined: 800; formula $C_{66}H_{65}F_6O_8P_4Rh_2S_2$ (two molecules), MM per molecule 747.0 g/mol; T = 200(2) K; triclinic, P-1 (No. 2, Z = 2); a = 1,149.5(1) pm; b = 1,515.5(1) pm; c = 2,049.6(2) pm; α = 71.784(1)°; β = 78.518(1)°; γ = 70.494(1)°; V = 3,179.2(5) × 10^6 pm^3; ρ (calc.) = 1.561 g/cm^3; Absorption coefficient = 0.758 mm^{-1}; F(000) = 1,522; Goof (F^2) = 1.035; crystal size = 0.8 × 0.8 × 0.6 mm^3; index ranges $-16 < h < 16$, $-21 < k < 20$, $-28 < l < 28$; completeness to θ = 28.34: 95.2 %; R_1 ($I > 2\sigma$) = 0.0316, wR_2 = 0.0851 (all data), largest difference peak and hole: 0.836 and −0.513 × 10^{-6} pm^{-3}. Structural details for **4***OTf*$CDCl_3$: Reflections collected/unique/observed: 25,128/9,067/8,250 [R(int) = 0.0317]; parameters refined: 467; formula $C_{37}H_{40}Cl_3F_3NO_3P_2RhS$, MM 906.96 g/mol; T = 200(2) K; monoclinic, Pn (No. 7, Z = 2); a = 1,158.8(3) pm; b = 944.1(3) pm; c = 1,815.7(5) pm; β = 105.465(5)°; V = 1,914(1) × 10^6 pm^3; ρ (calc.) = 1.573 g/cm^3; Absorption coefficient = 0.846 mm^{-1}; F(000) = 924; Goof (F^2) = 1.014; crystal size = 0.6 × 0.6 × 0.5 mm^3; index ranges $-15 < h < 15$, $-12 < k < 12$, $-24 < l < 24$; completeness to θ = 28.34: 97.7%; R_1 ($I > 2\sigma$) = 0.0307 wR_2 = 0.0698 (all data), largest difference peak and hole: 0.653 and −0.325 × 10^{-6} pm^{-3}.

3. Van Rooy A, Orij EN, Kamer PCJ, Van Leeuwen PWNM (1995) Organometallics 14:34
4. Van Rooy A, de Bruijn JNH, Roobeek KF, Kamer PCJ, Van Leeuwen PWNM (1996) J Organomet Chem 507:69
5. Van Leeuwen PWNM, Roobeek CF (1983) J Organomet Chem 258:343
6. Jongsma T, Challa G, Van Leeuwan PWNM (1991) J Organomet Chem 421:121
7. Van Rooy A, Orij EN, Kamer PCJ, Van Den Aardweg F, Van Leeuwen PWNM (1991) J Chem Soc Chem Commun 16:1096
8. Desset SL, Cole-Hamilton DJ (2009) Angew Chem Int Ed 49:1472
9. van der Slot SC, Kamer PCJ, van Leeuwen PWNM, Fraanje J, Goubitz K, Lutz M, Spek AL (2000) Organometallics 19:2504
10. Magee MP, Luo W, Hersh WH (2002) Organometallics 21:362
11. E. Piras, Dissertation no. 16317 (ETH Zürich, 2005)
12. Dahmen N, Griesheimer P, Makarczyk P, Pitter S, Walter O (2006) J Organomet Chem 690:1467
13. Kainz S, Koch D, Baumann W, Leitner W (1997) Angew Chem Int Ed Engl 36:1628
14. Koch D, Leitner W (1998) J Am Chem Soc 120:13398
15. Wong EH, Prasad L, Gabe EJ, Bradley FC (1982) J Organomet Chem 236:321
16. Bradley FC, Wong EH, Gabe EJ, Lee FL, Lepage Y (1987) Polyhedron 6:1103
17. Pavlik S, Mereiter K, Puchberger M, Kirchner K (2005) Organometallics 24:3561
18. Irvine DJ, Cole-Hamilton DJ, Barnes J, Hodgson PKG (1989) Polyhedron 8:1575
19. Irvine DJ, Glidewell C, Cole-Hamilton DJ, Barnes JC, Howie A (1991) J Chem Soc Dalton Trans 263:1765
20. Bravo J, Castro J, Garcia-Fontan S, Rodriguez-Martinez MC, Rodriguez-Seoane P (2006) Eur J Inorg Chem 3028
21. Domide D, Kaifer E, Mautz J, Walter O, Behrens S, Himmel HJ (2008) Eur J Inorg Chem 3177
22. Hoffmann R (1981) Science 211:95
23. Durap F, Biricik N, Gumgum B, Ozkar S, Ang WH, Fei Z, Scopelliti R (2008) Polyhedron 27:96
24. Gallo V, Mastrorilli P, Nobile CF, Braunstein P, Englert U (2006) Dalton Trans 8:2342
25. Gumgum B, Biricik N, Durap F, Ozdemir I, Gurbuz N, Ang WH, Dyson P (2007) J Appl Organomet Chem 21:11
26. Bowen LE, Haddow MF, Orpen AG, Wass DF (2007) Dalton Trans 1160
27. Simon-Manso E, Valderrama M (2006) J Organomet Chem 691:380
28. Valderrama M, Contreras R, Boys D (2003) J Organomet Chem 665:7
29. Posset T, Rominger F, Blümel J (2005) Chem Mater 17:586
30. Ewart G, Lane AP, McKechnie J, Payne DS (1964) J Chem Soc 1543
31. Yip SK, Lam WH, Zhu N, Yam VWW (2006) Inorg Chim Acta 359:3639
32. Balakrishna MS, Teipel S, Pinkerton AA, Cavell RG (2001) Inorg Chem 40:1802
33. Walter O, Huttner G, Kern R (1996) Z Naturforsch B 51:922
34. C. Claver, P.W. van Leeuwen, Rhodium Catalyzed Hydroformylation (Springer; 2000)
35. Maura R, Steele J, Vendier L, Arquier D, Bastin S, Urrutigoïty M, Kalck P, Igau A (2011) J Organomet Chem 696:897
36. Ionescu C (2009) Katalyse und Katalysatoren zur Hydroformylierung langkettiger Olefine in überkritischem Kohlendioxid. Dissertation, Universität Heidelberg
37. Gorschinski A, Habicht W, Walter O, Behrens S, Ionescu C, Powietzka B (in preparation)
38. Maniut C (2007), Reaktionstechnische Aspekte zur Hydroformylierung in überkritischem Kohlendioxid. Dissertation, Universität Heidelberg
39. F. Wurst, Überführung der Hydroformylierung mit immobilisierten Rhodium-Katalysatoren in ein kontinuierliches Verfahren im Labormaßstab. (Dissertation, Universität Heidelberg, to be concluded in 2013)
40. Heck RF, Breslow DS (1961) J Am Chem Soc 83:4023
41. Evans D, Yagupsky G, Wilkinson G (1968) J Chem Soc A 3133
42. SADABS, Siemens area detector absorption correction programme (Siemens, 1997)
43. SHELX-97, G. Sheldrick (University of Göttingen, Germany, 1997)
44. Xpma L, Zsolnai G (1997) Huttner. University of Heidelberg, Germany
45. Winray R, Soltek G (1997) Huttner. University of Heidelberg, Germany